Fusion Loop Peptide of the West Nile Virus Envelope Protein Is Essential for Pathogenesis and Is Recognized by a Therapeutic Cross-Reactive Human Monoclonal Antibody[1]

Hameeda Sultana,* Harald G. Foellmer,* Girish Neelakanta,* Theodore Oliphant,[§] Michael Engle,[¶] Michel Ledizet,[‡] Manoj N. Krishnan,* Nathalie Bonafé,[‡] Karen G. Anthony,[‡] Wayne A. Marasco,[‖] Paul Kaplan,[‡] Ruth R. Montgomery,[†] Michael S. Diamond,[§¶] Raymond A. Koski,[‡] and Erol Fikrig[2]*[#]

West Nile virus is an emerging pathogen that can cause fatal neurological disease. A recombinant human mAb, mAb11, has been described as a candidate for the prevention and treatment of West Nile disease. Using a yeast surface display epitope mapping assay and neutralization escape mutant, we show that mAb11 recognizes the fusion loop, at the distal end of domain II of the West Nile virus envelope protein. Ab mAb11 cross-reacts with all four dengue viruses and provides protection against dengue (serotypes 2 and 4) viruses. In contrast to the parental West Nile virus, a neutralization escape variant failed to cause lethal encephalitis (at higher infectious doses) or induce the inflammatory responses associated with blood-brain barrier permeability in mice, suggesting an important role for the fusion loop in viral pathogenesis. Our data demonstrate that an intact West Nile virus fusion loop is critical for virulence, and that human mAb11 targeting this region is efficacious against West Nile virus infection. These experiments define the molecular determinant on the envelope protein recognized by mAb11 and demonstrate the importance of this region in causing West Nile encephalitis. *The Journal of Immunology,* **2009, 183: 650–660.**

West Nile virus is an arthropod-borne positive-sense, ssRNA flavivirus that cycles between mosquitoes and birds (1, 2). The virus also infects humans, horses, and a variety of other vertebrates (3–5). In man, West Nile virus can cause a febrile illness and neurological disease that may result in paralysis and/or death (6, 7). West Nile virus is endemic in many parts of Africa and Asia, and was first introduced into North America in 1999 (8–12). During the past 9 years, West Nile virus has spread across the United States and into other neighboring countries (11). Treatment for West Nile virus infection is currently supportive, as effective vaccines and therapeutics have not yet been approved for use in humans.

West Nile virus is related to medically important flaviviruses, including dengue, Japanese encephalitis, yellow fever, and tick-borne encephalitis virus, among others (4, 5). Flaviviruses are small spherical virions encoding three structural (capsid, precursor membrane/membrane, and envelope (E)) and seven nonstructural proteins (13–15). The E protein has important roles in viral attachment to cells, fusion with endosomal compartments, and modulating host immune responses (16–18). The ectodomain of West Nile virus E protein folds into three structurally distinct domains (DI, DII, and DIII) forming head-to-tail homodimers on the surface of the virion (14, 16–18). DI is the central domain that organizes the entire E protein structure (18). DII is formed from two extended loops projecting from DI and lies in a pocket at the DI and DIII interface of the adjacent E protein in the dimer (17, 18). At the distal end of DII is a glycine-rich, hydrophobic sequence called the fusion loop, which encompasses residues 98–110, and is highly conserved among flaviviruses (16–19). This region has been implicated in the pH-dependent type II fusion event; during this process it becomes exposed and reoriented outward, making it available for membrane contact (17, 18). DIII forms a seven-stranded Ig-like fold, is the most membrane distal domain in the mature virion, and has been suggested to be involved in receptor binding (18). A 53-residue stem region links the ectodomain to a two-helix C-terminal transmembrane anchor that is important for virion assembly and fusion (17, 20, 21).

Current efforts are focused on identifying specific determinants on flaviviruses that facilitate the development of vaccines or therapeutics. Ab therapy has been shown to be effective in mice, both as prophylaxis and as a treatment for flavivirus infections (22, 23). Much of this protection in the polyclonal response is attributed to anti-E protein Abs, as passive immunization with E protein-specific antisera or mAbs protects mice from lethal West Nile virus challenge (18, 24–26). Some of these mouse Abs neutralized both West Nile and dengue viruses by binding to conserved epitopes in DI and DII (18, 26). Our group recently developed recombinant human single-chain variable region Ab fragments fused to an IgG1 Fc domain (scFvFc) against the West Nile virus E protein using a

*Section of Infectious Diseases and [†]Section of Rheumatology, Department of Internal Medicine, Yale University School of Medicine, New Haven, CT 06520; [‡]L2 Diagnostics, New Haven, CT 06511; [§]Department of Molecular Microbiology and Departments of [¶]Medicine, Pathology & Immunology, Washington University School of Medicine, St. Louis, MO 63130; [‖]Department of Cancer Immunology and AIDS, Dana Farber Cancer Institute, Boston, MA 02115; and [#]Howard Hughes Medical Institute, Chevy Chase, MD 20815

Received for publication January 12, 2009. Accepted for publication April 26, 2009.

The costs of publication of this article were defrayed in part by the payment of page charges. This article must therefore be hereby marked *advertisement* in accordance with 18 U.S.C. Section 1734 solely to indicate this fact.

[1] These studies were supported in part by National Institutes of Health Grants AI 070343, AI 50031, and AI061373. E.F. is an investigator of the Howard Hughes Medical Institute. The funding agencies had no role in conducting the study and in preparing the manuscript.

[2] Address correspondence and reprint requests to Dr. Erol Fikrig, Section of Infectious Diseases, Department of Internal Medicine, Yale University School of Medicine, S525A, 300 Cedar Street, New Haven, CT 06520-8022. E-mail address: erol.fikrig@yale.edu

www.jimmunol.org/cgi/doi/10.4049/jimmunol.0900093

phage display library screen, and we have evaluated the efficacy of these Abs both in vitro and in vivo (27). Five of these Abs protected mice from death when given before West Nile virus infection, and two Abs, including mAb11, provided substantial protection when administered to mice after viral challenge (27). mAb11 binding kinetic rates, affinity for recombinant West Nile virus E protein, and the comparisons with other scFvFcs were measured by surface plasmon resonance, where the K_d values showed an increase of approximately two orders of magnitude (in comparison to the scFvs), perhaps due to increased avidity of the bivalent scFvFc for the E protein (27). Seven of the scFvFcs, including mAb11, neutralized West Nile virus plaque formation by >80%; however, neutralization by scFvs was 10- to 20-fold less effective than by corresponding scFvFc proteins (27). mAb11 also cross-neutralized dengue virus in vitro and is therefore a potential candidate for an Ab therapeutic against flavivirus infections (27). In this study, we have generated an Ab escape mutant to mAb11 and defined the Ab-binding region on the E protein using a yeast display assay. Our studies reveal the importance of this epitope in viral pathogenesis and support development of the Ab as a therapeutic agent for West Nile and dengue virus infections.

Materials and Methods

Selection of a West Nile virus neutralization escape mutant using mAb11

To assess whether immunologic pressure promotes neutralization escape in vitro, the mouse neurovirulent wild-type West Nile virus strain CT 2741 was used for selection of antigenic variants. West Nile virus (100 PFU) was mixed with mAb11 at a concentration of 100 μg/ml. This concentration of mAb11 reduced nearly 50–60% of infection of the wild-type West Nile virus in Vero cells when tested in indirect immunofluorescence assay (data not shown). The Ab-virus complex was incubated for 1 h at room temperature before addition to Vero cells (African green monkey kidney cell line ATCC CCL-81) grown in DMEM plus 10% FBS, 1% L-glutamine, and 1% penicillin-streptomycin and incubated at 37°C in 5% CO_2. Viral supernatant was removed 48 h after infection, incubated with additional mAb11, and added to uninfected Vero cells. After three cycles of neutralization, the Ab concentrations were increased from 100 to 400 μg/ml (for two cycles of neutralization), then to 600 μg/ml (for five cycles of neutralization), and 800 μg/ml (for six cycles of neutralization). Escape mutants were treated stringently with higher mAb11 concentrations to select dominant isolates. RT-PCR and sequence analysis revealed that out of 14 isolates, 7 showed a clearly dominant population of the mutant virus, whereas 7 others had a mixed population of wild-type West Nile virus and the neutralization escape mutant (data not shown). All dominant isolates analyzed contained both amino acid substitutions in the E protein of the same isolate. The dominant isolates with mutations were then plaque-purified by plating on Vero cells as described (27). The final neutralization dominant isolate selected for this study was designated as HSF11.

Sequence analysis

Total RNA was extracted using a QIAamp Viral RNA Mini kit (Qiagen). Reverse transcription was conducted using the iScript cDNA synthesis kit (Bio-Rad). PCR reactions were performed with the specific primers shown in supplemental Table S1.[3] The fragments generated from the respective primer combinations were sequenced from both ends. DNA sequencing was performed by the Keck DNA sequencing facility at Yale University. The base pair changes were confirmed with chromatographs. Alignment of the wild-type E protein fusion loop (aa 98–110) and the transmembrane domain regions (aa 476–488) with the deduced amino acid substitutions in HSF11 were analyzed using Lasergene DNASTAR software.

RT-PCR analysis

PCR primers were designed to confirm the mutations g317t-bp and c1451t-bp in the envelope gene of the mAb11 neutralization escape mutants (supplemental Table S1). The mutant forward primer (RT-PCR HSF11; shown in supplemental Table S1) had base pair changes at the end of the primer sequence in comparison to the wild-type primer sequence (RT-PCR Wild type). This change enabled specific PCR amplification of viral cDNA sequences containing the g317t mutation. The reverse primer (E gene reverse primer) was common for both wild-type and mutant PCR reactions. E gene forward/reverse primer pair was used to amplify the E gene fragment outside the mutation region and used as an internal control. PCR at extensions (62°C) with either wild-type or mutant primer pairs showed a band only with wild-type or mutant virus, respectively. HSF11 had a dominant mutant population and was amplified only with the mutant-specific primers. RT-PCR reactions without a template were used as a negative control.

Western blot analysis and protein expression

Vero cells (2×10^5) were infected with either wild type or HSF11 at a multiplicity of infection of 1, and both the viral supernatant and cell pellet fractions were processed for Coomassie staining (to analyze the total protein profile) and Western blot analysis. Total lysate (20 μg) was separated by SDS-PAGE (12%) and probed with mAb11 at a concentration of 0.3–1 μg/ml (under nonreducing conditions) or E protein polyclonal antisera at 1/2000 dilution (under reducing conditions) followed by anti-human or anti-rabbit IgG secondary Abs (Sigma-Aldrich), respectively. Production of mAb11 was previously described (27). To determine mAb11 cross-reactivity, 10 μg of purified West Nile and dengue virus (DENV)[4] (serotypes 1–4) truncated E proteins (domains I–III expressed in *Drosophila* S2 cells) were probed with mAb11 at a concentration of 0.3–1 μg/ml, followed by anti-human IgG secondary Ab.

To determine the mAb11 cross-reactivity with tick-borne encephalitis virus (TBEV), a synthetic gene encoding the 401 N-terminal amino acids of the TBEV E ectodomain preceding three stop codons was synthesized, which was expressed in frame with the BiP signal sequence and downstream of the metallothionein promoter of the *Drosophila* expression vector (Invitrogen). The recombinant plasmid was cotransfected into *Drosophila* S2 cells along with pCoHygro plasmid (Invitrogen) encoding a hygromycin resistance marker for selection of stable transfectants (the transfected cells were cultivated for 6 wk in the presence of hygromycin to obtain a population of stable transfectants). Expression of TBEV E gene in this cell population was induced with copper sulfate. One to 10 μg/ml of mAb11 was used to probe a lysate of *Drosophila* S2 cells stably expressing truncated TBEV E protein after induction (uninduced and untransfected *Drosophila* S2 cells were used as controls).

Twenty micrograms of total mouse brain homogenates was probed with E protein polyclonal rabbit antisera, followed by anti-rabbit secondary Ab or anti-mouse IgG (HRP-conjugated) to detect H and L chains as markers for permeability. Actin served as loading control. ECL detection of Ab binding was performed with the ECL Western blotting detection system (Amersham).

Plaque assays

One to 2 days before infection, Vero and/or C6/36 mosquito cells were seeded in 6-well plates at a density 2×10^5 cells/ml. Stock of wild-type West Nile virus and/or HSF11 with known PFU was diluted in DMEM medium. Serial dilutions of the viruses were incubated with Vero (1–4 h at 37°C) and mosquito cells (1–4 h at 30°C) in 5% CO_2 and the plates were shaken every 15 min. Agar overlay was prepared by mixing equal volumes of a solution consisting of 100 ml of 2× MEM (Invitrogen)/DMEM with sterile 2% agar/0.4% agarose, 4% neutral red/0.3 volume of MTT solution (Sigma-Aldrich) and antimycotic/antibiotic was added to the above mix just before adding the overlay. Agar overlay was added and the plates were incubated for 4–5 days at 37°C in 5% CO_2 and plaques were counted at 5×10^1 PFU dilution to determine the differences in viral replication/titers.

Yeast library screen for selection of random mutants

The West Nile virus envelope protein-domain I–II mutant library was constructed as described previously (18, 26). The library was screened with mAb11 labeled with Alexa Fluor 647 to identify loss-of-binding mutants as described (18, 26). mAb E113 that binds outside the fusion loop served as control. Yeast cells were sorted on the single Ab-negative population. This population was enriched through three rounds of sorting, and individual colonies were tested for loss of binding by flow cytometry analysis. Plasmids were recovered using a Zymoprep yeast miniprep kit (Zymo Research), transformed into DH5α-competent cells (Stratagene), and sequenced.

[3] The online version of this article contains supplemental material.

[4] Abbreviations used in this paper: DENV, dengue virus; i.c., intracranial; qRT-PCR, quantitative RT-PCR; TBEV, tick-borne encephalitis virus.

Mice infection and survival studies

C57BL/6 mice were purchased from Charles River Laboratories. All West Nile virus challenge experiments were performed with 6-wk-old females. Groups of 5–10 mice were inoculated i.p. with 10^3 PFU of wild-type West Nile virus strain CT 2741 or 10^3, 10^4, and 10^5 PFU of HSF11 isolate in 200 μl of PBS with 1% gelatin. Based on previous studies, mice infected with West Nile virus typically die at 6–12 days postinfection due to CNS invasion by the virus (28, 29). Survival of mice was monitored daily for West Nile virus-associated symptoms, and mortality until 25 days postinfection and survival data are from three independent experiments. Surviving mice were either euthanized or, in selected experiments, mice were dissected to harvest tissues (brain, blood, and spleen). All animal experiments were done in accordance with the Yale University Animal Care and Use Committee regulations. Neurovirulence of dengue 2 serotype (DENV2) (New Guinea C strain) virus was evaluated in 3- to 4-wk-old BALB/c mice in groups of 10. Mice were inoculated i.p. with 800 μg of mAb11 one day before intracranial (i.c.) administration of 150,000 PFU of DENV2. For dengue virus 4 serotype (DENV4) mouse infection studies, 3- to 4-wk-old BALB/c mice in groups of 21 (PBS control) or 18 (mice inoculated i.p. with 800 μg of mAb11 one day before DENV4 infection) were challenged i.c. with 50 PFU of DENV4 strain H241. Mice were under observation for a period of 30 days for survival recordings. Survival data summarize results of three independent experiments. All dengue virus animal experiments were approved and performed in accordance with Washington University Animal Studies Committee guidelines.

Evaluation of the blood-brain barrier permeability

Blood-brain barrier leakage was evaluated as described (28, 29). Briefly, C57BL/6 mice were challenged (i.p.) with 10^3 or 10^4 PFU of wild-type West Nile virus or HSF11 isolate. At day 4 postinfection, mice were injected i.p. with 800 μl of 1% (w/v) Evans blue dye, perfused with PBS 1 h later, and brains were excised and evaluated macroscopically for leakage of Evans blue dye.

Infection of in vitro cell lines

Vero, C6/36 *A. albopictus*, mouse cerebrospinal microvascular endothelial, human HEK 293, and mouse neuroblastoma (N2a) cell lines were obtained from the American Type Culture Collection. Cell lines were maintained as described by the distributor. We established the mouse primary cultures of cortical and spinal cord neurons from brains of day 16 (E16) C57BL/6 mouse embryos as described (28–31). Primary neurons and other cell lines were seeded on 6-, 12-, or 24-well plates at cell densities of 2×10^5, 10^5, or 10^4 cells/ml, respectively, incubated for 24 h at 37°C and infected with wild-type West Nile virus or HSF11 (multiplicity of infection of 1–10). Cell lysates were collected for analysis by quantitative RT-PCR (qRT-PCR) analysis. For mAb11 in vitro cell line protection assays 800 μg/ml mAb11 was preincubated (1 h, room temperature) with either HSF11 or wild-type parental virus and the mixture was incubated with the cells for respective times (as shown in the Figs.). Duplicate samples were collected per data point from three independent experiments.

Monocyte isolation and mAb11 protection assay

PBMCs were isolated from a healthy donor with no acute illness, taking no antibiotics or nonsteroidal anti-inflammatory drugs, and previously screened for exposure to West Nile virus or dengue infection. Blood was collected in accordance with the regulations of Human Investigation Committee of Yale University. PBMCs were isolated by Ficoll-Hypaque density gradient centrifugation and suspended in RPMI 1640 medium containing 10% FBS, 2 mM glutamine, 1000 U/ml penicillin, and 1000 μg/ml streptomycin (Invitrogen). Cells were plated at 3×10^6 density, and nonadherent cells were removed after 2 h with PBS washes. Cells were infected (at MOI of 2) with either DENV2 (New Guinea strain) or DENV2 preincubated with 800 μg/ml mAb11 (1 h, room temperature). Cells were harvested in duplicates on days 1–3 for extraction of total RNA and qRT-PCR analysis.

qRT-PCR analysis

To determine the viral burden, TLR3 expression, and cytokine mRNA levels, total RNA was extracted from either cell cultures or frozen tissues using RNeasy extraction kit (Qiagen), and cDNA was synthesized from 1 μg RNA using the iScript cDNA synthesis kit (Bio-Rad). qRT-PCR was performed using previously published primers for West Nile virus *E* (28), DENV2 *capsid* (supplemental Table S1), *IFN-α*, *TNF-α, IL-6, IL-12p40* (28–31), and *TLR3* (28). Primers for β-actin cDNA were used in parallel with the primers for qRT-PCR normalization. Equal amounts of mouse/human monocytes cDNA samples were used in parallel for β-actin and West Nile virus *E* gene/DENV2 *capsid* gene qRT-PCR analysis. The ratio of West Nile virus *E* gene copy or DENV2 *capsid* gene copy/β-actin gene copy was used as an index to determine the infection rate of each sample.

Immunofluorescence and confocal microscopy

Microscope slides containing fixed, permeabilized Vero cells infected with various flaviviruses/arboviruses and uninfected controls were purchased from Panbio. Immunofluorescence was performed as described (32). Briefly, slides were incubated with 25 μl of 50 μg/ml mAb11 or the isotype control IgG in PBS containing 1% BSA. We also performed staining with mAb 4G2, which also defines its target epitope in the conserved flavivirus fusion sequence as positive control to further ensure similar growth of these viruses (data not shown). Slides were incubated overnight at 4°C in a moist chamber, rinsed in PBS, and stained for anti-human secondary Ab conjugated with Alexa 594 (Molecular Probes). The slides were rinsed in PBS and counterstained with 20 μg/ml 4′,6-diamidino-2-phenylindole (Molecular Probes). Images were acquired using an LSM 510 laser scanning confocal microscope (Zeiss) as previously described (33).

Recombinant proteins and ELISAs

Truncated, soluble versions of recombinant E proteins from West Nile virus and dengue virus serotypes 1–4 were produced and purified as described previously (15, 32). ELISA for mAb11 cross-reactivity was performed with recombinant E proteins from dengue virus serotypes 1–4 and West Nile virus (150 ng/well) as described previously (32).

Statistical analysis

Error bars define mean (±SD) values. Statistical significance between the values was determined using nonpaired Student's *t* test. To assess statistical differences between survival rates, we performed a log-rank test (Prism; GraphPad Software).

Results

Selection of a West Nile virus isolate that is resistant to mAb11

Passive transfer of mAb11 protects mice from West Nile virus encephalitis when administered before, and after, viral challenge (27). A West Nile virus isolate resistant to mAb11 was generated to determine the mAb11 binding epitope on the West Nile virus *E* protein, and to understand its importance in virulence. West Nile virus was incubated with mAb11 in cell culture, as outlined in the *Materials and Methods*, and a clone resistant to the neutralizing effects of mAb11 was isolated. This clone, designated HSF11, had amino acid substitutions at G106V and T484M, and it was used in subsequent studies. The G106V mutation is in the viral fusion loop located at amino acid positions 98–110 of the E protein (Fig. 1*A*). This region is highly conserved among flaviviruses, consistent with its fundamental role in the viral life cycle (19). The T484M mutation lies in the transmembrane domain of the E protein, which likely participates in the maturation of the initial polyprotein and virion assembly (Fig. 1*A*). RT-PCR analysis, with primers specific for either the wild-type or mutant virus, confirmed that HSF11 was a dominant isolate (Fig. 1*B*).

The binding of mAb11 to HSF11 was then analyzed by immunoblot. mAb11 binds recombinant or virion-associated wild-type West Nile virus E protein under nonreducing conditions, suggesting that the Ab-binding epitope is conformational and not linear (27). As expected, mAb11 does not react with E protein from mutant HSF11 virions under nonreducing conditions (Fig. 1*C*). However, both wild-type West Nile virus and HSF11 reacted with polyclonal E protein antisera under reducing conditions (Fig. 1*C*).

To determine the kinetics of infection of HSF11 compared with the parental wild-type strain, Vero cells or C6/36 *A. albopictus* mosquito cells were infected with the viruses, and efficiency of viral growth was determined by qRT-PCR of West Nile virus *E* gene. The in vitro growth kinetics of HSF11 and wild-type West Nile virus in Vero cells were similar (Fig. 1*D*) at both early and later time points of infection. In contrast, HSF11 had an ~3-fold lower infection rate that was found to be significant at both early

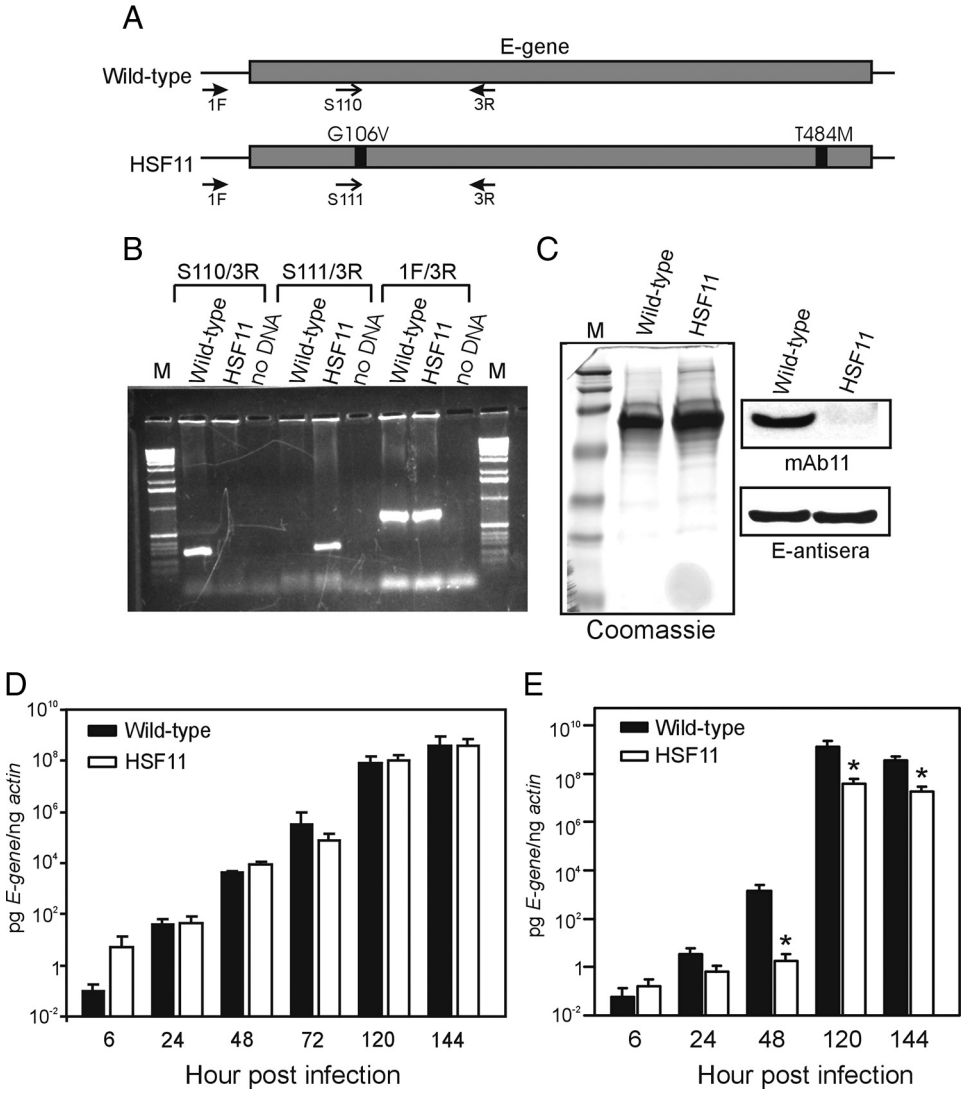

FIGURE 1. Characterization of HSF11 a West Nile virus isolate resistant to the neutralizing effects of mAb11. *A*, Schematic representation of the West Nile virus *E* gene, with primers used for RT-PCR to confirm the mutation in the HSF11 E protein fusion loop. Arrows represent the direction of the primer. *B*, RT-PCR with the primers shown in *A*. M indicates the 1-kb DNA ladder. RT-PCR reactions without template were used as a negative control (no DNA). *C*, HSF11 does not bind mAb11. Shown is the Coomassie-stained gel of concentrated Vero cell supernatants containing the viral particles (wild-type West Nile virus or HSF11); 20 μg of the viral supernatants were probed with mAb11 or E protein antisera in immunoblots. Infection kinetics in Vero (*D*) and *A. albopictus* (*E*) cells of wild-type West Nile virus and HSF11 were quantified by qRT-PCR with *E* gene-specific primers relative to actin. Shown are the results from three independent experiments, performed in triplicate. $*$, $p < 0.05$ between wild-type virus and HSF11. Error bars represent the SD from the mean.

and later days of mosquito cell infection when compared with control West Nile virus (Fig. 1*E*). These data suggest that infectivity patterns in mammals and arthropods may require a different mode of attachment, entry, or fusion. Indeed, mechanisms of viral entry/fusion may be different in mosquito cells compared with mammalian cells (34, 35). Viral replication was further characterized by plaque assays that yielded similar results in Vero cells infected with wild-type West Nile or HSF11, with known PFU of viruses (supplemental Fig. 1*A*). HSF11 yielded similar plaque sizes in both Vero and mosquito cells (data not shown). However, in mosquito cells, HSF11 yielded significantly lower plaque numbers in comparison to cells infected with wild-type West Nile virus (supplemental Fig. 1*B*).

To establish the binding site of mAb11 for West Nile virus E protein, we used a negative selection yeast surface display flow cytometric assay in which the gene for the West Nile virus E

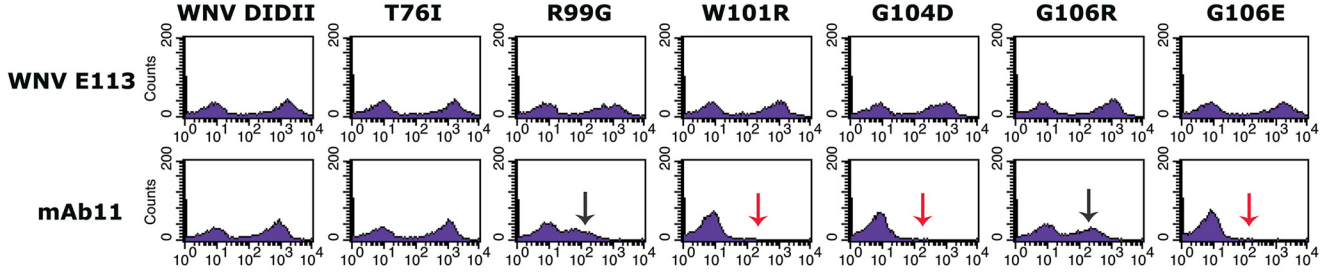

FIGURE 2. Yeast display selection of E protein variants that do not bind mAb11. Amino acid residues required for mAb11 binding were mapped using a yeast display assay, with negative selection of random mutants, and flow cytometry. Yeast displaying domain I (DI) and DII regions were tested for binding to E113 and mAb11. Representative histograms are shown for mAb11 and E113 (a West Nile virus-specific mAb that binds the hinge interface between DI and DII (26)). Mutations in the fusion loop abolish or reduce mAb11 binding. Red arrows denote mutations resulting in loss of binding, and blue arrows denote the reduction in the percentage of binding. These data are representative of three independent experiments. Counts are from log fluorescence intensity on the FL4 (660 nm) channel.

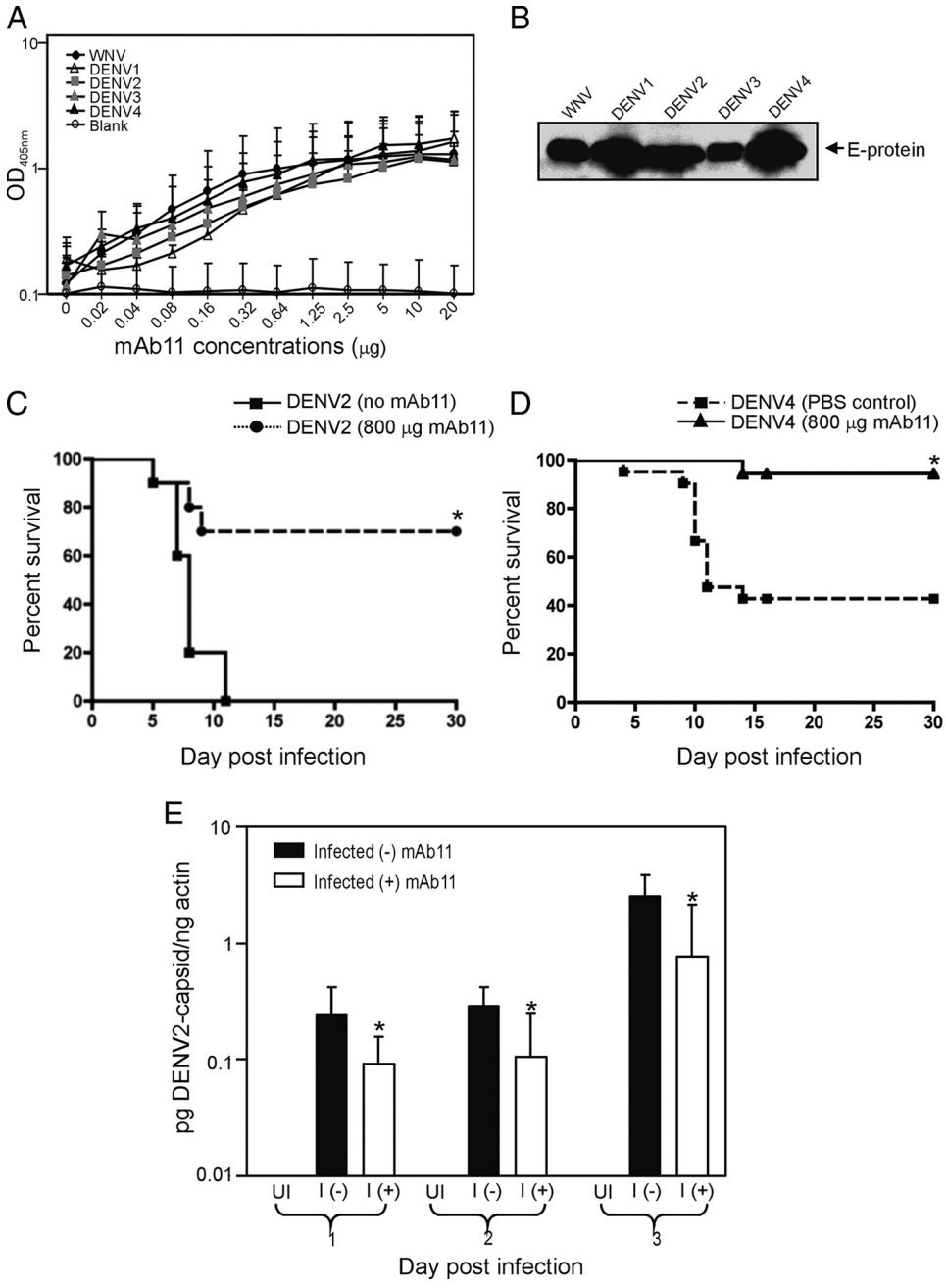

FIGURE 3. mAb11 cross-reacts with and protects against dengue viruses. *A*, ELISA binding assay shows the mAb11 cross-reactivity with recombinant dengue E proteins (serotypes 1–4). mAb11 shows efficient cross-reactivity with the dengue E proteins (all four serotypes) in a dose-dependent manner. West Nile virus E protein serves as the positive control and no protein serves as negative control. *B*, A representative Western blot analysis showing the efficient cross-reactivity of mAb11 (1 μg/ml) with all four serotypes of dengue E proteins (purified recombinant E proteins). West Nile virus E protein serves as positive control. *C* and *D*, mAb11 protects mice from DENV2 and DENV4 infections. Mice were inoculated i.p. with 800 μg of mAb11 one day before i.c. infection with DENV2 or DENV4. $*$, $p < 0.02$ (DENV2) and $p < 0.0009$ (DENV4) survival difference between DENV2- and DENV4-infected mice in comparison to the control animals. *E*, mAb11 protects primary human monocytes from DENV2 infection. Monocytes isolated from a healthy donor were infected with DENV2 and either treated with 800 μg of mAb11 or left untreated. Human monocytes were significantly protected by mAb11 from DENV2 infection (days 1–3). $*$, $p < 0.05$ between untreated and mAb11-treated cells.

protein was subjected to random mutagenesis (18). As previous studies had suggested that mAb11 reacted with yeast expressing only DI–DII(27), we mapped the amino acid residues required for mAb11 binding by using a mutant library of $\sim 10^5$ DI–DII variants. Single amino acid substitutions located in the highly conserved fusion loop abolished (W101R, G104D, and G106E) or reduced (G106R) the binding of mAb11 to West Nile virus E DI–DII on yeast (Fig. 2). Notably, mAb11 binding was not appreciably altered with yeast that expressed 24 other single amino acid mutations in DI and DII that affected previously described neutralizing mAbs against West Nile virus (18) (data not shown).

As the target-binding site of mAb11 is the fusion loop, a region of the E protein that is highly conserved among flaviviruses, it may have utility as a therapeutic agent for diverse flaviviral infections. Using immunofluorescence staining of virally infected Vero cells, we have determined that mAb11 cross-reacts with some of the related flaviviruses, including dengue, St. Louis encephalitis,

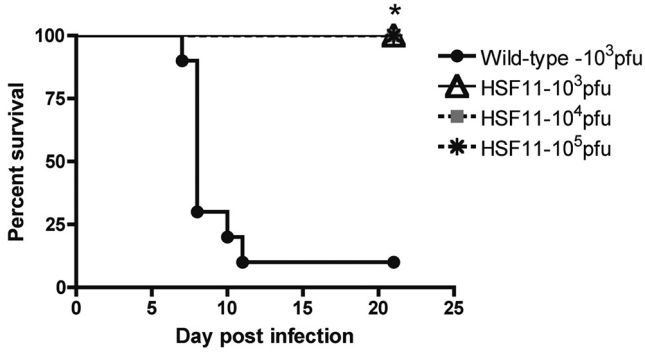

FIGURE 4. HSF11 does not cause lethal infection in mice. Survival of C57BL/6 mice challenged with 10^3 PFU of wild-type West Nile virus or 10^3, 10^4, and 10^5 PFU of HSF11 isolate. Groups infected with 10^3 PFU of wild-type virus or HSF11 had 20 animals per group, and mice infected with 10^4 and 10^5 PFU of HSF11 had 10 animals per group. $*$, $p < 0.05$ between HSF11- and wild-type virus-infected mice.

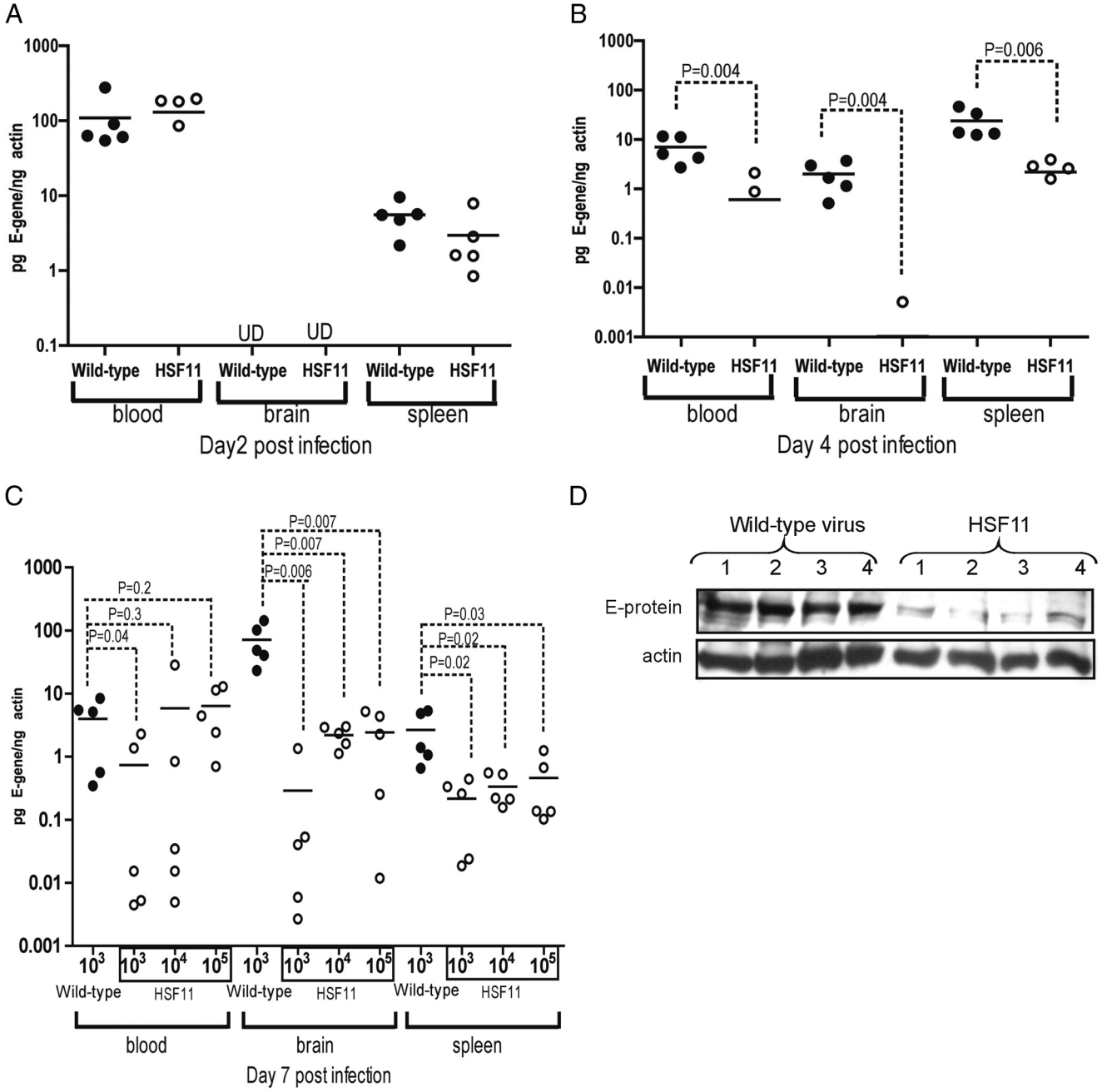

FIGURE 5. HSF11 is less neuroinvasive than wild-type West Nile virus. Viral loads in selected tissues of mice inoculated with 10^3, 10^4, and 10^5 PFU of HSF11 or 10^3 PFU of wild-type West Nile virus. Each group contained five animals examined at day 2, 4, or 7 after viral challenge (*A–C*). UD, undetectable. Data are representative of results obtained in three independent experiments, performed in triplicate. *D*, Immunoblot of the E protein levels in HSF11- and wild-type West Nile virus-infected mice brains on day 7. Actin serves as the loading control.

yellow fever, Japanese encephalitis, and Murray Valley encephalitis viruses (supplemental Table S2 and supplemental Fig. S2). Furthermore, we found that mAb11 showed no cross-reactivity with Venezuelan equine encephalitis virus, Western equine encephalitis, and La Crosse viruses (supplemental Table S2 and supplemental Fig. S2). Recombinant TBE envelope protein also showed no cross reactivity with mAb11 (data not shown). Binding assays including ELISA and immunoblots using recombinant E proteins confirmed that mAb11 cross-reacts with all four dengue serotypes (1–4) (Fig. 3, *A* and *B*). To determine the cross-therapeutic potential of mAb11, we inoculated mice with 800 μg of mAb11 one day before i.c. infections with New Guinea C strain dengue virus serotype 2 (150,000 PFU; DENV2) or H241 strain dengue virus serotype 4 (50 PFU; DENV4). We found that mAb11 was markedly protective in vivo against infections with either DENV2 or DENV4 when given 1 day before infection (Fig. 3, *C* and *D*). Furthermore, we found that mAb11 provides significant protection in an in vitro model of human dengue infection using primary monocytes from a healthy donor (Fig. 3*E*).

HSF11 is infectious, but does not cause lethal encephalitis, in mice

The virulence of HSF11 was assessed in the murine model of West Nile encephalitis. As expected, animals infected with an i.p. dose of 10^3 PFU of wild-type West Nile virus developed encephalitis and died within 2 wk (Fig. 4). In contrast, mice challenged (i.p.)

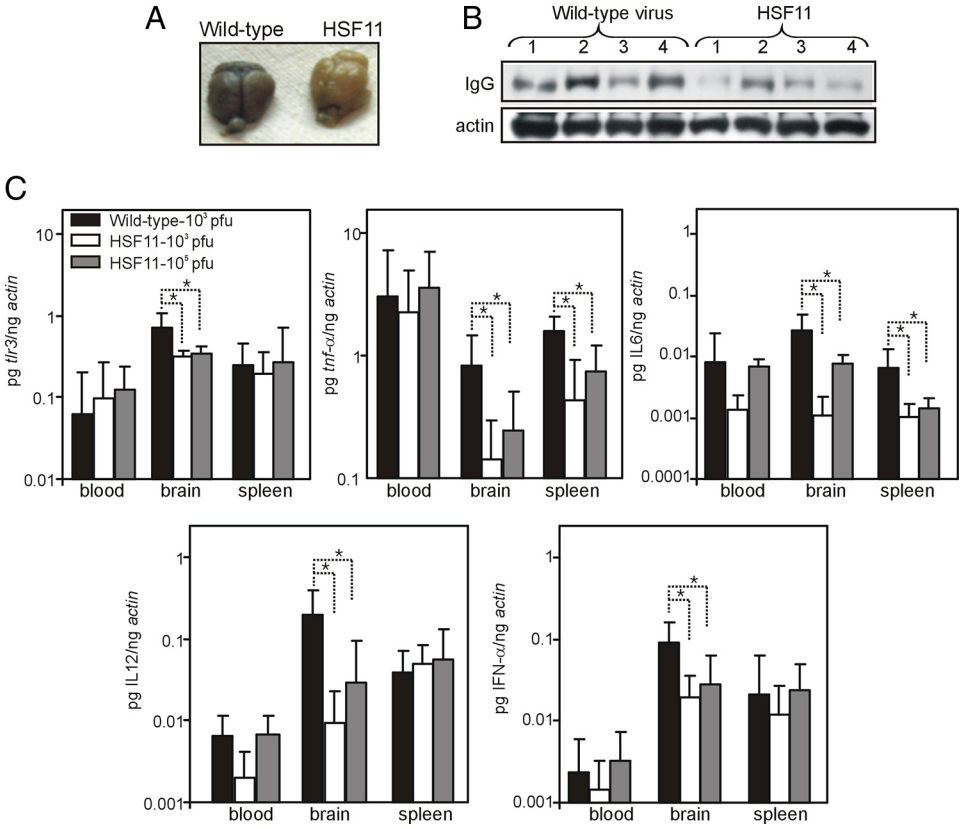

FIGURE 6. HSF11 does not substantially alter blood-brain barrier permeability. *A*, Evans blue dye staining of HSF11- or wild-type West Nile virus-infected mouse brains. *B*, Immunoblot of IgG (H chain) in HSF11- or wild-type West Nile virus-infected brains. Actin serves as the loading control. *C*, TLR3, TNF-α, IL-6, IL-12, and IFN-α mRNA levels in the blood, brain, and spleen of HSF11- and wild-type West Nile virus-infected mice at day 7. Both groups of mice were infected with 10^3 PFU of either HSF11 or wild-type West Nile virus or 10^5 PFU of HSF11 isolate. Results are from five mice per group and two independent experiments, performed in triplicate. $*$, $p < 0.05$.

with 10^3, 10^4, or 10^5 PFU of HSF11 did not develop a lethal infection and showed no deaths, indicating that the mutant virus was less pathogenic than the parental viral isolate (Fig. 4). Our infection doses were selected to reveal the full range of pathology of the HSF11 and wild-type West Nile virus strains. qRT-PCR demonstrated that on day 2 postinfection there was no significant difference in viral load in blood or spleens of mice infected with 10^3 PFU of HSF11 or wild-type West Nile virus (Fig. 5*A*). However, on days 4 and 7 postinfection, mice infected with 10^3 PFU of HSF11 had a lower viral load in the blood, brain, and spleen than did mice infected with similar doses of wild-type West Nile viruses (Fig. 5, *B* and *C*). These data suggest that HSF11 may be cleared by the host immune response after day 2 postinfection. Animals challenged with 10^4 or 10^5 PFU of HSF11 developed a similar degree of viremia in blood as mice infected with 10^3 PFU of wild-type West Nile virus (Fig. 5*C*). These HSF11-infected animals, however, still had lower levels of virus in the brain than did mice infected with 10^3 PFU of wild-type West Nile virus, suggesting that HSF11 has a diminished capacity for neuroinvasion or is attenuated for neurovirulence (Fig. 5*C*). Accordingly, a lower amount of E protein was detected by immunoblots of brains of HSF11-infected mice (10^3 PFU) at day 7 postinfection compared with animals infected with wild-type West Nile virus (Fig. 5*D*). The immunoblots were consistent with the reduced viral levels as demonstrated by qRT-PCR. The nucleotide substitutions in HSF11 from the mouse brains were stable and showed no evidence of reversion to the wild-type parental virus on day 7 postinfection (data not shown).

Blood-brain barrier permeability is associated with viral neuroinvasion, and it was therefore evaluated by administering Evans blue dye to mice infected with HSF11 or wild-type West Nile virus. There was considerably more leakage of the dye into the CNS of mice infected (i.p.) with 10^3 PFU of wild-type West Nile virus compared with animals infected with a similar dose of HSF11 (Fig. 6*A*). Examination of IgG levels in brain of these two groups of mice, which is also indicative of blood-brain barrier permeability, yielded similar results (Fig. 6*B*). The significant reduction in brain viral loads of mice infected with even higher infectious doses (10^4 or 10^5 PFU) of HSF11 also correlated with reduced leakage of the blood-brain barrier permeability in brains of those mice (data not shown). These data suggest that HSF11 may be impaired in permeabilizing the blood-brain barrier.

TLR (*TLR3*) binding to the dsRNA inside virally infected cells leads to the production of antiviral and inflammatory cytokines such as IFN-α, IL-12, IL-6, and TNF-α (28). It has been shown that *TLR3*-mediated responses can potentially facilitate West Nile virus entry into the CNS by altering the blood-brain barrier permeability (28). We therefore quantified *TLR3* mRNA levels in blood, brain, and spleens of mice challenged with HSF11. On day 4 postinfection, the blood-brain barrier is already significantly compromised and virus is detected in brains of mice infected with wild-type West Nile virus (28). Early in infection (day 4 postinfection), *tlr3* and IL-6 mRNA levels were significantly lower in the spleens of mice infected with HSF11 compared with the controls, although, no differences were seen in the brains of these mice (supplemental Fig. 3). *Tlr3* mRNA levels were also significantly lower at day 7 in brains of HSF11-infected mice (10^3 and 10^5 PFU) in comparison to animals infected with 10^3 PFU of wild-type West Nile virus (Fig. 6*C*). Additionally, mRNA levels of the proinflammatory cytokines TNF-α, IL-6, IL-12, and IFN-α (which have been shown to play a role in blood-brain barrier permeability (28)) were also reduced in brains (day 7 postinfection) of mice infected with 10^3 and 10^5 PFU of HSF11, although no significant difference was observed in these cytokine mRNA levels in blood at day 7 postinfection (Fig. 6*C*). Furthermore, at day 7 postinfection, TNF-α and IL-6 mRNA levels were also significantly reduced in spleens of mice infected with 10^3 and 10^5 PFU of HSF11 (Fig. 6*C*). These data demonstrate that HSF11 has a reduced ability to

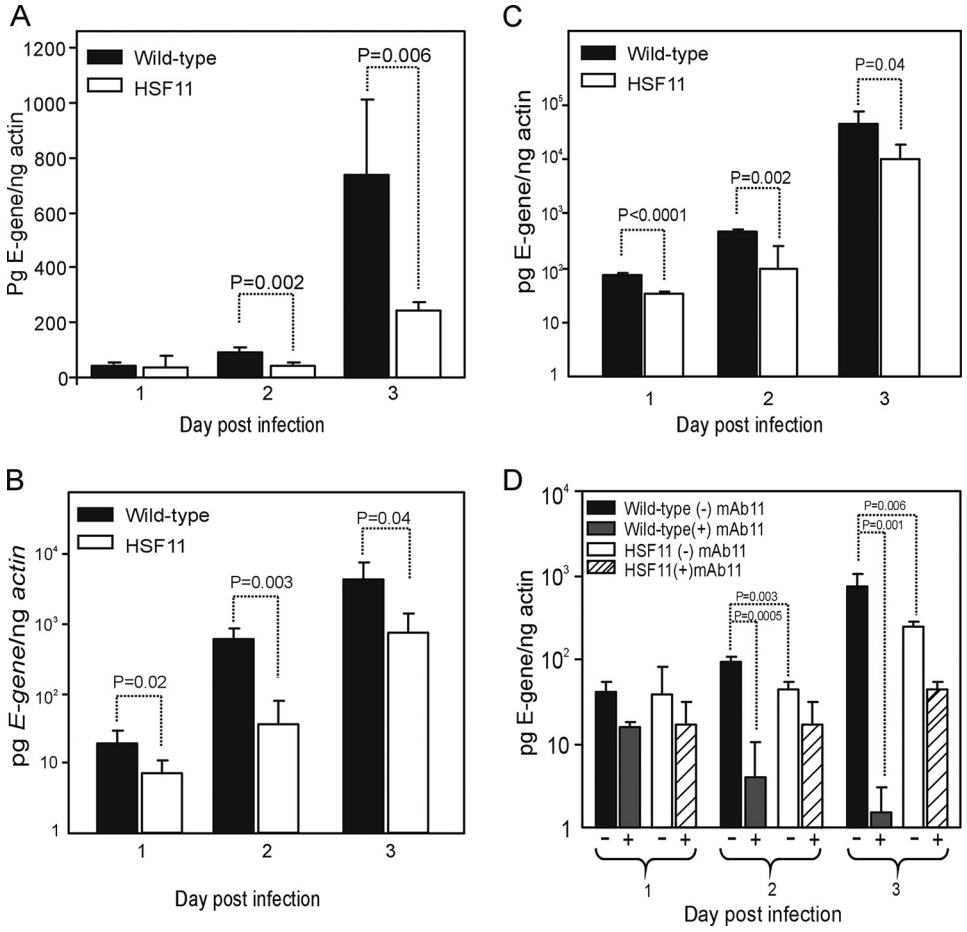

FIGURE 7. HSF11 has diminished infectivity in cells associated with the CNS. Kinetics of HSF11 infection in murine brain microvascular endothelial cells (*A*) and cortical (*B*) and spinal cord (*C*) neuronal cell cultures showed lower HSF11 loads in comparison to the controls. The viral burden was quantified by qRT-PCR on days 1, 2, and 3, respectively, and was normalized to actin mRNA levels. *D*, mAb11 reduces wild-type West Nile virus infection in brain microvascular endothelial cells. All results are from three independent experiments, performed in triplicate. Error bars indicate SD from the mean.

induce blood-brain barrier permeability and the cytokine release associated with this inflammation process.

HSF11 has a diminished ability to infect cells in the CNS

The blood-brain barrier is composed of specialized microvascular endothelial cells in association with astrocyte foot processes. Studies were therefore performed to determine whether HSF11 has a decreased ability, compared with wild-type West Nile virus, to infect cells associated with the CNS. Experiments used cell lines in vitro, so that infectivity could be fully dissociated from the influence of viral load on the blood-brain barrier. The HSF11 viral levels were significantly lower compared with wild-type West Nile virus upon infection of a brain microvascular endothelial cell line in vitro (Fig. 7*A*). The viral burden of primary murine cortical and spinal cord neurons infected with HSF11 was also significantly diminished in comparison to the parental West Nile virus (Fig. 7, *B* and *C*). The wild-type virus-infected brain microvascular endothelial cells incubated with mAb11 had lower viral loads than did controls, suggesting that mAb11 protects in vitro cultures of mouse microvascular endothelial cells from wild-type West Nile virus infection (Fig. 7*D*). Mouse primary cortical neuronal cells incubated with mAb11 also had significant lower viral loads in comparison to the controls (data not shown). Although HSF11 had diminished ability to infect neuronal cells, it was competent to infect these cells, as indicated by the increase in viral loads over time (from day 1 to day 3 postinfection). Mouse neuroblastoma (N2a) cells also showed reduced infection kinetics with HSF11 in comparison to the parental West Nile virus controls (data not shown). These data suggest that HSF11 has a decreased capacity to infect brain microvascular endothelial, N2a, and primary neuronal cells, in contrast to its unaltered capacity to infect Vero and human embryonic kidney (HEK 293) cells (data not shown). The differential infectivity between wild-type parental West Nile virus and HSF11 suggest a specific defect in neuronal infectivity of the mutant (HSF11) viral strain.

Discussion

The present study identified the conformational epitope on the West Nile virus E protein that mAb11 recognizes, highlights the importance of this region in viral pathogenesis, and implicates this region as a therapeutic target. A yeast display assay demonstrated that mutations in the E protein fusion loop abolished binding of mAb11, thereby suggesting the domain II fusion loop as the primary recognition site for this recombinant human mAb. Selection and sequencing of a West Nile virus neutralization escape mutant (HSF11) confirmed that mAb11 recognized an epitope on the E protein fusion loop. HSF11 contained a Gly→Val substitution at position 106 within the E protein fusion loop and a Thr→Met alteration at position 484 in the distantly placed transmembrane domain of the E protein. All antigenic variants that were isolated had both mutations (G106V and T484M) in the E protein. Substitution of Val for Gly[106] is a nonconserved amino acid change that results in increased hydrophobicity of the Cys-Gly-Leu tripeptide sequence, corresponding to residues 105–107 in the fusion loop (36, 37). During the E protein conformational transition, the fusion loops clusters at one end of an elongated trimeric molecule. The C-terminal segments connected to the viral transmembrane region align with the sides of the E protein trimer, pointing toward the fusion loop (13, 15, 17, 37). We speculate that in this configuration the fusion loop and the transmembrane domain are spatially close

and may result in the T484M mutation (if 484 is a bona fide recognition site) that may either influence the binding of mAb11 to a complex conformational epitope involving the fusion loop or may compensate in part for G106V mutation in the conserved fusion loop. This unique conformational epitope may potentially make mAb11 a better candidate for use as a therapeutic than other neutralizing, cross-reactive Abs. Taken together, these data suggest that mAb11 binds a conformationally dependent epitope involving the fusion loop.

HSF11 is infectious but attenuated in its ability to invade the CNS and cause encephalitis, demonstrating that an intact fusion loop is critical for viral pathogenesis. On day 2 postinfection, no significant differences in viral loads (blood and spleens) were found from mice infected with 10^3 PFU of HSF11 or wild-type parental virus, indicating that HSF11 is infectious and not defective for replication in vivo. However, as infection progressed, HSF11 viral loads declined dramatically over days 4 and 7 postinfection, suggesting that the mutant strain may be more readily cleared by the host immune response. Also, HSF11 was not able to efficiently penetrate the blood-brain barrier and invade the CNS, even with high inocula of virus (10- and 100-fold higher), which resulted in a peripheral viremia similar to that found in mice administered with wild-type West Nile virus (10^3 PFU). The blood-brain barrier, a structural component of the brain vasculature, serves important protective functions and is composed of specialized microvascular endothelial cells in association with astrocyte foot processes (38, 39). The reduced ability of HSF11 to infect the in vitro cerebrospinal microvascular endothelial cells was associated with diminished leakiness of the blood-brain barrier in HSF11-infected mice. HSF11 also demonstrated decreased infectivity of primary mouse neurons, but it did not seem to be defective for replication, as the viral loads gradually increased over time from day 1 to day 3 postinfection. The differences in infection kinetics/replication characteristics of HSF11 may depend on the mode of entry, membrane fusions, different mechanisms of viral absorption and/or penetration, and the involvement of variable surface receptors or host cell factors required for viral infection and replication in these different cell culture systems in vitro. We found that mAb11 also significantly reduced wild-type parental virus infection of cerebrospinal microvascular endothelial and mouse primary neuronal cells (in vitro), suggesting that mAb11 would be therapeutic during late stages of infection and may provide protection even after West Nile virus has crossed the blood-brain barrier. Overproduction of proinflammatory cytokines, such as TNF-α, enhances neuroinvasion and injury during West Nile virus infection (28). Our study also shows that HSF11 is impaired in inducing the TNF-α-mediated proinflammatory response, which may reduce HSF11 neurovirulence. Our data suggest that this is one possible mechanism by which HSF11 is less pathogenic and attenuated for neuroinvasion. These data indicate that brisk inflammatory responses to West Nile virus, and efficient viral entry and infection of the brain, are dependent on an intact E protein fusion loop and the fusion activity.

Flaviviruses enter cells by fusing their membranes with the host cell membrane (receptor-mediated endocytosis) or at an internal site after uptake by endocytosis (40–42). The viral envelope protein undergoes a triggered conformational change upon binding to a receptor or exposure to the acidic environment of the endosome that exposes the buried portion of the E protein, the fusion loop peptide, to insert the fusion peptide into the target host membrane (16, 37, 40–42). It has been shown that the flavivirus fusion loop directly participates in the low pH-induced membrane fusions (16, 37, 42). Exposure to acidic pH accompanying the fusion process initiates highly orchestrated conformational changes. Thus, the amino acid change in the conserved fusion peptide that reduces the fusion of viral and host membranes is of great significance (16, 17, 19). Recombinant subviral particles of TBEV E protein that contain Asp or Phe for Leu^{107} substitution in the fusion peptide have been shown to be defective for membrane fusion (37, 40–42). A DENV-2 fusion loop antigenic variant is shown to lower the pH threshold for fusion in infected C6/36 mosquito cells (36). The mode of entry and fusion processes may be different for mosquito and mammalian cells, as HSF11-infected *A. albopictus* mosquito cells showed significantly lower viral infectivity and plaque formation, suggesting that HSF11 entry or fusion might be delayed or defective in mosquito cells. The differential infectivity of HSF11 suggests that HSF11 may have impaired membrane fusion ability in mosquito cells.

The differences in pathogenesis of HSF11 compared with wild-type West Nile virus suggest that the fusion loop may be a potential target for antiviral therapy. Our studies show that mAb11 cross reacts with multiple flaviviruses (including dengue, St. Louis encephalitis, yellow fever, Japanese encephalitis, and Murray Valley encephalitis viruses). The cross-reactivity of mAb11 with all four dengue serotypes in vitro, the in vitro DENV2 protection studies with human monocytes, and in vivo cross-protection of mice against DENV2 and DENV4 infections indicate that mAb11 is a potential therapeutic to treat both dengue and West Nile virus infections. Monocytes have been shown to be the principal target cells for dengue virus infection among human PBMCs (43), and the in vitro model of DENV2 infection of human monocytes suggested mAb11 to be protective against human dengue virus infections. Human dengue infections are typically not neuroinvasive and may be less sensitive to mAb11 therapy than in the i.c. mouse model, but there are limitations of the mouse model with i.c. DENV administration. Equine polyclonal anti-West Nile virus Abs selected for binding to a fusion loop were cross-reactive with dengue E proteins (32). The fusion loop has previously been shown to be important in E protein recognition by some neutralizing mAbs, as mutations in the fusion loop reduce the binding of mouse and primate neutralizing mAbs against West Nile and dengue viruses (18, 26, 36, 44–50). Abs that recognize flavivirus fusion peptide epitopes have been previously described as broadly cross-reactive but weakly neutralizing Abs (18, 26, 37). Neutralization and protective potential of West Nile virus E protein DI- or DII-specific mAbs was less than that of DIII-specific neutralizing mAbs (18). Nonetheless, all of these neutralizing mAbs protected mice when administered before West Nile virus infection (18). The differences in the neutralization efficiencies between DI- or DII-specific mAbs to that of DIII-specific mAbs could be attributed to the stoichiometric requirements of the Ab binding to the epitope or neutralization by different mechanisms (51). Trainor et al. have recently identified amino acids involved in flavivirus cross-reactive epitope determinants using an extensive mutagenesis of E protein cross-reactive epitopes in St. Louis encephalitis E protein (52). Mutations in the highly conserved amino acids in the fusion loop (substitutions at E protein residues Gly^{104}, Gly^{106}, and Leu^{107}) produced variations in the cross-reactive mAb reactivity (52, 53). Our experiments indicate that Gly^{106} is not only required for binding of mAb11, which has a broad and high degree of cross-reactivity, but also plays a central role in flavivirus infectivity and pathogenesis and that mutation in this highly conserved region would compromise virulence.

The murine model of West Nile virus infection partially reflects human disease. The vast majority of the experimentally infected mice succumb to lethal West Nile encephalitis, while only a small percentage (1–5%) of patients with West Nile virus infection develop neurologic disease. Pathology in experimental animals has

some similarities to human disease, including infection and injury of brain stem, hippocampal, and spinal cord neurons (54). In a subset of immunocompetent animals, West Nile virus is largely cleared from the serum and peripheral organs by the end of first week and is subsequently followed by infection of the CNS (28, 54). In mice, viremia is directly correlated with early West Nile virus entry into the CNS by crossing the blood-brain barrier (28, 29, 54–58). West Nile virus may cross the blood-brain barrier by multiple mechanisms (28, 29, 55–59), for example, by migrating into the brain in infected immune cells, by infection of olfactory neurons and spread to the olfactory bulb, by entering the spinal cord via axonal retrograde transport along peripheral neurons, by traversing endothelial tight junctions, and by directly infecting microvascular endothelial cells. Additionally, infection of human brain microvascular endothelial cells modulates tight junction proteins and cell adhesion molecules, thereby facilitating West Nile virus-infected leukocyte entry into the CNS (60). In an in vitro blood-brain barrier model comprised of human brain microvascular endothelial cells, West Nile virus infection was transient and resulted in transmigration of cell-free West Nile virus across the barrier without compromising the blood-brain barrier integrity. Transient human brain microvascular endothelial infection without cytopathic effects may explain why West Nile virus has not been detected in human brain endothelial cells at later stages of infection (60). Additional studies will determine the similarities between West Nile virus infection in experimental models and humans.

Collectively, these data demonstrate that an intact West Nile virus fusion loop is critical for virulence, and that mAb11 targeting this region is efficacious against West Nile virus. The recombinant human Ab mAb11 can be produced rapidly, is free of blood-borne pathogens, and targets the highly conserved fusion loop of the flavivirus E proteins, making it an ideal candidate for Ab therapy. As mAb11 is efficacious in mice that have established West Nile virus infection (27) and provides protection to microvascular endothelial and neuronal cells, it is also possible that this Ab may be therapeutic in patients that have developed early CNS disease. Future studies and clinical trials will help address these issues.

Acknowledgments

We thank Dr. John Anderson for parental West Nile virus isolate CT 2741, Dr. Yorgo Modis for dengue 3 serotype recombinant envelope protein, Dr. Brett Lindenbach for helpful discussions, and Debby Beck and Lin Zhang for technical assistance.

Disclosures

The authors have no financial conflicts of interest.

References

1. Anderson, J. F., T. G. Andreadis, C. R. Vossbrinck, S. Tirrell, E. M. Wakem, R. A. French, A. E. Garmendia, and H. J. Van Kruiningen. 1999. Isolation of West Nile virus from mosquitoes, crows, and a Cooper's hawk in Connecticut. *Science* 286: 2331–2333.
2. Komar, N., S. Langevin, S. Hinten, N. Nemeth, E. Edwards, D. Hettler, B. Davis, R. Bowen, and M. Bunning. 2003. Experimental infection of North American birds with the New York 1999 strain of West Nile virus. *Emerg. Infect. Dis.* 9: 311–322.
3. Bunning, M. L., R. A. Bowen, B. Cropp, K. Sullivan, B. Davis, N. Komar, M. Godsey, D. Baker, D. Hettler, D. Holmes, and C. J. Mitchell. 2001. Experimental infection of horses with West Nile virus and their potential to infect mosquitoes and serve as amplifying hosts. *Ann. NY Acad. Sci.* 951: 338–339.
4. Mackenzie, J. S., D. J. Gubler, and L. R. Petersen. 2004. Emerging flaviviruses: the spread and resurgence of Japanese encephalitis: West Nile and dengue viruses. *Nat. Med.* 10: 98–109.
5. Mukhopadhyay, S., R. J. Kuhn, and M. G. Rossmann. 2005. A structural perspective of the flavivirus life cycle. *Nat. Rev. Microbiol.* 3: 13–22.
6. Marfin, A. A., and J. D. Gubler. 2001. West Nile encephalitis: an emerging disease in the United States. *Emerg. Infect. Dis.* 33: 1713–1719.
7. Hayes, E. B., J. J. Sejvar, S. R. Zaki, R. S. Lanciotti, A. V. Bode, and G. L. Campbell. 2005. Virology, pathology, and clinical manifestations of West Nile virus disease. *Emerg. Infect. Dis.* 11: 1174–1179.
8. Komar, N. West Nile virus: epidemiology and ecology in North America. 2003. *Adv. Virus Res.* 61: 185–234.
9. Beasley, D. W., C. T. Davis, H. Guzman, D. L. Vanlandingham, A. P. Travassos da Rosa, R. E. Parsons, S. Higgs, R. B. Tesh, and A. D. Barrett. 2003. Limited evolution of West Nile virus has occurred during its southwesterly spread in the United States. *Virology* 309: 190–195.
10. Briese, T., X. Y. Jia, C. Huang, L. J. Grady, and W. I. Lipkin. 1999. Identification of a Kunjin/West Nile-like flavivirus in brains of patients with New York encephalitis. *Lancet* 354: 1261–1262.
11. Gould, L. H., and E. Fikrig. 2004. West Nile virus: a growing concern? *J. Clin. Invest.* 113: 1102–1107.
12. Lanciotti, R. S., J. T. Roehrig, V. Deubel, J. Smith, M. Parker, K. Steele, B. Crise, K. E. Volpe, M. B. Crabtree, J. H. Scherret, et al. 1999. Origin of the West Nile virus responsible for an outbreak of encephalitis in the northeastern United States. *Science* 286: 2333–2337.
13. Bressanelli, S., K. Stiasny, S. L. Allison, E. A. Stura, S. Duquerroy, J. Lescar, F. X. Heinz, and F. A. Rey. 2004. Structure of a flavivirus envelope glycoprotein in its low-pH-induced membrane fusion conformation. *EMBO J.* 23: 728–738.
14. Nybakken, G. E., C. A. Nelson, B. R. Chen, M. S. Diamond, and D. H. Fremont. 2006. Crystal structure of the West Nile virus envelope glycoprotein. *J. Virol.* 80: 11467–11474.
15. Modis, Y., S. Ogata, D. Clements, and S. C. Harrison. 2004. Structure of the dengue virus envelope protein after membrane fusion. *Nature* 427: 313–319.
16. Heinz, F. X., and S. L. Allison. 2001. The machinery for flavivirus fusion with host cell membranes. *Curr. Opin. Microbiol.* 4: 450–455.
17. Kanai, R., K. Kar, K. Anthony, L. H. Gould, M. Ledizet, E. Fikrig, W. A. Marasco, R. A. Koski, and Y. Modis. 2006. Crystal structure of west Nile virus envelope glycoprotein reveals viral surface epitopes. *J. Virol.* 80: 11000–11008.
18. Oliphant, T., G. E. Nybakken, M. Engle, Q. Xu, C. A. Nelson, S. Sukupolvi-Petty, A. Marri, B. E. Lachmi, U. Olshevsky, D. H. Fremont, et al. 2006. Antibody recognition and neutralization determinants on domains I and II of West Nile virus envelope protein. *J. Virol.* 80: 12149–12159.
19. Seligman, S. J. 2008. Constancy and diversity in the flavivirus fusion peptide. *Virol. J.* 5: 27.
20. Rey, F. A., F. X. Heinz, C. Mandl, C. Kunz, and S. C. Harrison. 1995. The envelope glycoprotein from tick-borne encephalitis virus at 2 Å resolution. *Nature* 375: 291–298.
21. Orlinger, K. K., V. M. Hoenninger, R. M. Kofler, and C. W. Mandl. 2006. Construction and mutagenesis of an artificial bicistronic tick-borne encephalitis virus genome reveals an essential function of the second transmembrane region of protein E in flavivirus assembly. *J. Virol.* 80: 12197–12208.
22. Engle, M. J., and M. S. Diamond. 2003. Antibody prophylaxis and therapy against West Nile virus infection in wild-type and immunodeficient mice. *J. Virol.* 77: 12941–12949.
23. Ben-Nathan, D., S. Lustig, G. Tam, S. Robinzon, S. Segal, and B. Rager-Zisman. 2003. Prophylactic and therapeutic efficacy of human intravenous immunoglobulin in treating West Nile virus infection in mice. *J. Infect. Dis.* 188: 5–12.
24. Goncharova, E., E. Ryzhikov, V. Poryvaev, L. Bulychev, N. Karpyshev, A. Maksyutov, and A. B. Ryzhikov. 2006. Intranasal immunization with inactivated tick-borne encephalitis virus and the antigenic peptide 89–119 protects mice against intraperitoneal challenge. *Int. J. Med. Microbiol.* 40: 195–201.
25. Wang, T., J. F. Anderson, L. A. Magnarelli, S. Bushmich, S. Wong, R. A. Koski, and E. Fikrig. 2001. West Nile virus envelope protein: role in diagnosis and immunity. *Ann. NY Acad. Sci.* 951: 325–327.
26. Oliphant, T., G. E. Nybakken, S. K. Austin, Q. Xu, J. Bramson, M. Loeb, M. Throsby, D. H. Fremont, T. C. Pierson, and M. S. Diamond. 2007. Induction of epitope-specific neutralizing antibodies against West Nile Virus. *J. Virol.* 81: 11828–11839.
27. Gould, L. H., J. Sui, H. Foellmer, T. Oliphant, T. Wang, M. Ledizet, A. Murakami, K. Noonan, C. Lambeth, K. Kar, et al. 2005. Protective and therapeutic capacity of human single-chain Fv-Fc fusion proteins against West Nile virus. *J. Virol.* 79: 14606–14613.
28. Wang, T., T. Town, L. Alexopoulou, J. F. Anderson, E. Fikrig, and R. A. Flavell. 2004. Toll-like receptor 3 mediates West Nile virus entry into the brain causing lethal encephalitis. *Nat. Med.* 10: 1366–1373.
29. Arjona, A., H. G. Foellmer, T. Town, L. Leng, C. McDonald, T. Wang, S. J. Wong, R. R. Montgomery, E. Fikrig, and R. Bucala. 2007. Abrogation of macrophage migration inhibitory factor decreases West Nile virus lethality by limiting viral neuroinvasion. *J. Clin. Invest.* 117: 3059–3066.
30. Lucas, M., T. Mashimo, M. P. Frenkiel, D. Simon-Chazottes, X. Montagutelli, P. E. Ceccaldi, J. L. Guenet, and P. Despres. 2003. Infection of mouse neurons by West Nile virus is modulated by the interferon-inducible 2′-5′ oligoadenylate synthetase 1b protein. *Immunol. Cell Biol.* 81: 230–236.
31. Tan, J., T. Town, D. Paris, T. Mori, Z. Suo, F. Crawford, M. P. Mattson, R. A. Flavell, and M. Mullan. 1999. Microglial activation resulting from CD40-CD40L interaction after β-amyloid stimulation. *Science* 286: 2352–2355.
32. Ledizet, M., K. Kar, H. G. Foellmer, N. Bonafe, K. G. Anthony, L. H. Gould, S. L. Bushmisch, E. Fikrig, and R. A. Koski. 2007. Antibodies targeting linear determinants of the envelope protein protect mice against West Nile virus. *J. Infect. Dis.* 196: 1741–1748.
33. Kong, K. F., K. Delroux, X. Wang, F. Qian, A. Arjona, S. E. Malawista, E. Fikrig, and R. R. Montgomery. 2008. Dysregulation of TLR3 impairs the innate immune response to West Nile virus in the elderly. *J. Virol.* 82: 7613–7623.

34. Hase, T., P. L. Summers, K. H. Eckels, and W. B. Baze. 1987. An electron and immunoelectron microscopic study of dengue-2 virus infection of cultured mosquito cells: maturation events. *Arch. Virol.* 92: 273–291.
35. Hase, T., P. L. Summers, K. H. Eckels, and W. B. Baze. 1987. Maturation process of Japanese encephalitis virus in cultured mosquito cells in vitro and mouse brain cells in vivo. *Arch. Virol.* 96: 135–151.
36. Goncalvez, A. P., R. H. Purcell, and C. J. Lai. 2004. Epitope determinants of a chimpanzee Fab antibody that efficiently cross-neutralizes dengue type 1 and type 2 viruses map to inside and in close proximity to fusion loop of the dengue type 2 virus envelope glycoprotein. *J. Virol.* 78: 12919–12928.
37. Stiasny, K., S. Kiermayr, H. Holzmann, and F. X. Heinz. 2006. Cryptic properties of a cluster of dominant flavivirus cross-reactive antigenic sites. *J. Virol.* 80: 9557–9568.
38. Morrey, J. D., A. L. Olsen, V. Siddharthan, N. E. Motter, H. Wang, B. S. Taro, D. Chen, D. Ruffner, and J. O. Hall. 2008. Increased blood-brain barrier permeability is not a primary determinant for lethality of West Nile virus infection in rodents. *J. Gen. Virol.* 89: 467–473.
39. Olsen, A. L., J. D. Morrey, D. F. Smee, and R. W. Sidwell. 2007. Correlation between breakdown of the blood-brain barrier and disease outcome of viral encephalitis in mice. *Antiviral Res.* 75: 104–112.
40. Heinz, F. X., and S. L. Allison. 2000. Structures and mechanisms in flavivirus fusion. *Adv. Virus. Res.* 55: 231–269.
41. Stiasny, K., and F. X. Heinz. 2006. Flavivirus membrane fusion. *J. Gen. Virol.* 87: 2755–2766.
42. Allison, S. L., J. Schalich, K. Stiasny, C. W. Mandl, C. Kunz, and F. X. Heinz. 1995. Oligomeric rearrangement of tick-borne encephalitis virus envelope proteins induced by an acidic pH. *J. Virol.* 69: 695–700.
43. Kou, Z., M. Quinn, H. Chen, W. W. Rodrigo, R. C. Rose, J. J. Schlesinger, and X. Jin. 2008. Monocytes, but not T or B cells, are the principal target cells for dengue virus (DV) infection among human peripheral blood mononuclear cells. *J. Med. Virol.* 80: 134–146.
44. Goncalvez, A. P., R. Men, C. Wernly, R. H. Purcell, and C. J. Lai. 2004. Chimpanzee Fab fragments and a derived humanized immunoglobulin G1 antibody that efficiently cross-neutralize dengue type 1 and type 2 viruses. *J. Virol.* 78: 12910–12918.
45. Zhang, S., L. Li, S. E. Woodson, C. Y. Huang, R. M. Kinney, A. D. Barrett, and D. W. Beasley. 2006. A mutation in the envelope protein fusion loop attenuates mouse neuroinvasiveness of the NY99 strain of West Nile virus. *Virology* 353: 35–40.
46. Allison, S. L., J. Schalich, K. Stiasny, C. W. Mandl, and F. X. Heinz. 2001. Mutational evidence for an internal fusion peptide in flavivirus envelope protein E. *J. Virol.* 75: 4268–4275.
47. Nybakken, G. E., T. Oliphant, S. Johnson, S. Burke, M. S. Diamond, and D. H. Fremont. 2005. Structural basis of West Nile virus neutralization by a therapeutic antibody. *Nature* 437: 764–769.
48. Lok, S. M., V. Kostyuchenko, G. E. Nybakken, H. A. Holdaway, A. J. Battisti, S. Sukupolvi-Petty, D. Sedlak, D. H. Fremont, P. R. Chipman, J. T. Roehrig, et al. 2008. Binding of a neutralizing antibody to dengue virus alters the arrangement of surface glycoproteins. *Nat. Struct. Mol. Biol.* 15: 312–317.
49. Lai, C. Y., W. Y. Tsai, S. R. Lin, C. L. Kao, H. P. Hu, C. C. King, H. C. Wu, G. J. Chang, and W. K. Wang. 2008. Antibodies to envelope glycoprotein of dengue virus during the natural course of infection are predominantly cross-reactive and recognize epitopes containing highly conserved residues at the fusion loop of domain II. *J. Virol.* 82: 6631–6643.
50. Crill, W. D., and J. T. Roehrig. 2001. Monoclonal antibodies that bind to domain III of dengue virus E glycoprotein are the most efficient blockers of virus adsorption to Vero cells. *J. Virol.* 75: 7769–7773.
51. Pierson, T. C., Q. Xu, S. Nelson, T. Oliphant, G. E. Nybakken, D. H. Fremont, and M. S. Diamond. 2007. The stoichiometry of antibody-mediated neutralization and enhancement of West Nile virus infection. *Cell Host Microbe* 1: 135–145.
52. Trainor, N. B., W. D. Crill, J. A. Roberson, and G. J. Chang. 2007. Mutation analysis of the fusion domain region of St. Louis encephalitis virus envelope protein. *Virology* 360: 398–406.
53. Crill, W. D., N. B. Trainor, and G. J. Chang. 2007. A detailed mutagenesis study of flavivirus cross-reactive epitopes using West Nile virus-like particles. *J. Gen. Virol.* 88: 1169–1174.
54. Samuel, M. A., and M. S. Diamond. 2006. Pathogenesis of West Nile virus infection: a balance between virulence, innate and adaptive immunity, and viral evasion. *J. Virol.* 80: 9349–9360.
55. Diamond, M. S., and R. S. Klein. 2004. West Nile virus: crossing the blood-brain barrier. *Nat. Med.* 10: 1294–1295.
56. Klein, R. S., and M. S. Diamond. 2008. Immunological headgear: antiviral immune responses protect against neuroinvasive West Nile virus. *Trends Mol. Med.* 14: 286–294.
57. Wang, P., J. Dai, F. Bai, K. F. Kong, S. J. Wong, R. R. Montgomery, J. A. Madri, and E. Fikrig. 2008. Matrix metalloproteinase 9 facilitates West Nile virus entry into the brain. *J. Virol.* 82: 8978–8985.
58. Dai, J., P. Wang, F. Bai, T. Town, and E. Fikrig. 2008. Icam-1 participates in the entry of West Nile virus into the central nervous system. *J. Virol.* 82: 4164–4168.
59. Town, T., F. Bai, T. Wang, A. T. Kaplan, F. Qian, R. R. Montgomery, J. F. Anderson, R. A. Flavell, and E. Fikrig. 2009. Toll-like receptor 7 mitigates lethal West Nile encephalitis via interleukin 23-dependent immune cell infiltration and homing. *Immunity* 30: 242–253.
60. Verma, S., Y. Lo, M. Chapagain, S. Lum, M. Kumar, U. Gurjav, H. Luo, A. Nakatsuka, and V. R. Nerurkar. 2009. West Nile virus infection modulates human brain microvascular endothelial cells tight junction proteins and cell adhesion molecules: transmigration across the in vitro blood-brain barrier. *Virology* 385: 425–433.

Supplementary Figure Legends

Figure S1. Growth analysis of HSF11 by plaque assays. (A) Four days after infection of Vero cells, parental wild type West Nile virus and HSF11 variant produced similar numbers of plaques. (B) Under the same conditions, the HSF11 variant significantly yielded lower numbers of plaques than the parental wild type West Nile virus in C6/36 mosquito cells. Shown are the results from 5 independent experiments, performed in duplicates. * indicates statistically significant ($p < 0.05$) differences between parental wild-type West Nile virus and HSF11. Error bars represent the standard deviation from the mean.

Figure S2. mAb11 shows cross-reactivity with the related flaviviruses. Indirect immunofluorescence assay (IFA) data showing the cross-reactivity of mAb11 with representative flaviviruses –dengue (DENV), yellow fever (YFV), St. Louis encephalitis virus (SLEV), Japanese encephalitis virus (JEV) and Powassan (POW). Vero cells infected with the indicated arboviruses were purchased from PANBIO (USA). Cells were incubated with mAb11 (50 µg/ml; 25 µl of this stock was spotted on the PANBIO slides containing Vero cells infected with flaviviruses). Images were acquired using a laser scanning confocal microscope and visualized with anti-human IgG secondary antibody conjugated with Alexa 594 (Red = virus). Human IgG isotype control, uninfected Vero cells, Venezuelan equine encephalitis (VEE), Western equine encephalitis (WEE) and La Crosse (LAC) viruses served as negative controls for mAb11 staining. The IFA showed that mAb11 cross-reacts differently against a panel of flavivirus-infected Vero cells. Images were acquired with similar channel settings. The intensity of the signal was compared to that obtained with the isotype and uninfected controls.

Figure S3. TLR3 and cytokine responses are reduced in spleens of mice challenged with HSF11. TLR3 (A), TNF-α (B), IL-6 (C), IL-12 (D) and IFN-α (E), mRNA levels in spleen were determined at day4 post infection after intraperitoneal administration of 10^3 pfu of either wild type or HSF11 viruses. In HSF11 infected mice, tlr3 and IL-6 levels were significantly lower in spleens at day4 post infection. No differences were observed in brains of these mice. Shown are the Q-RT-PCR results from 5 mice per group obtained in 2 independent experiments. * indicates statistically significant values of the comparison ($P<0.05$, Student t test). Errors bars represent standard deviation from the mean value.

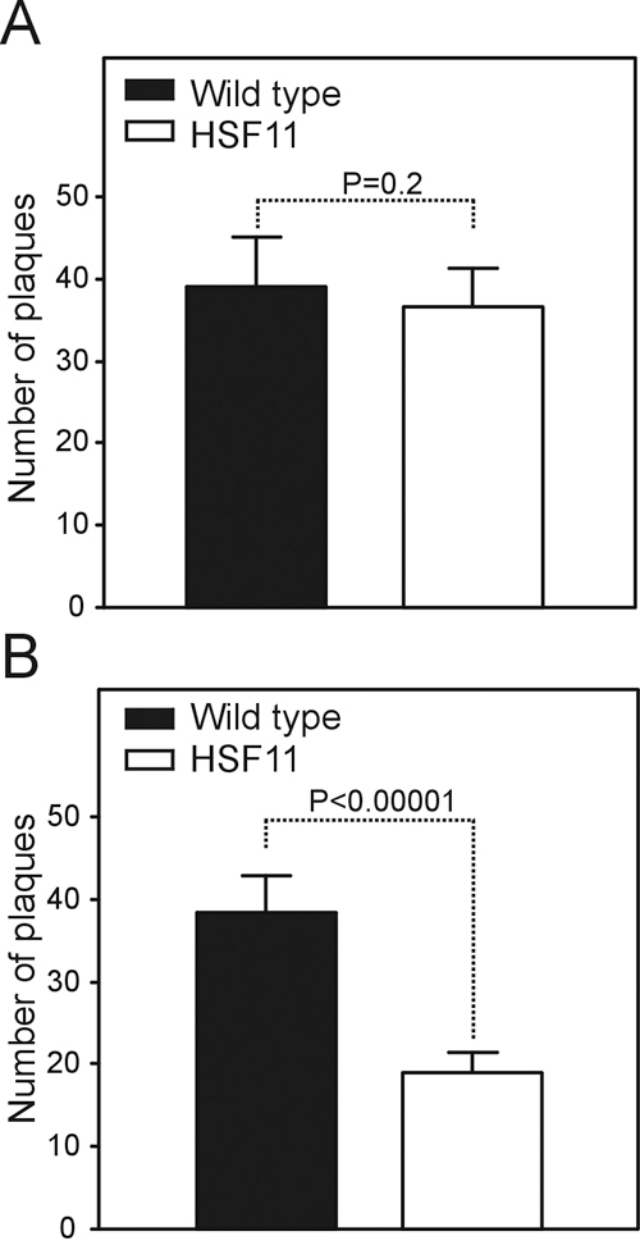
A
Wild type
HSF11
P=0.2
Number of plaques
50
40
30
20
10
0
B
Wild type
HSF11
P<0.00001
Number of plaques
50
40
30
20
10
0

Figure S1

Isotype-control
mAb11
WNV
YFV
JEV
VEE
LAC
Isotype-control
mAb11
DENV
SLEV
POW
WEE
Vero cells

Figure S2

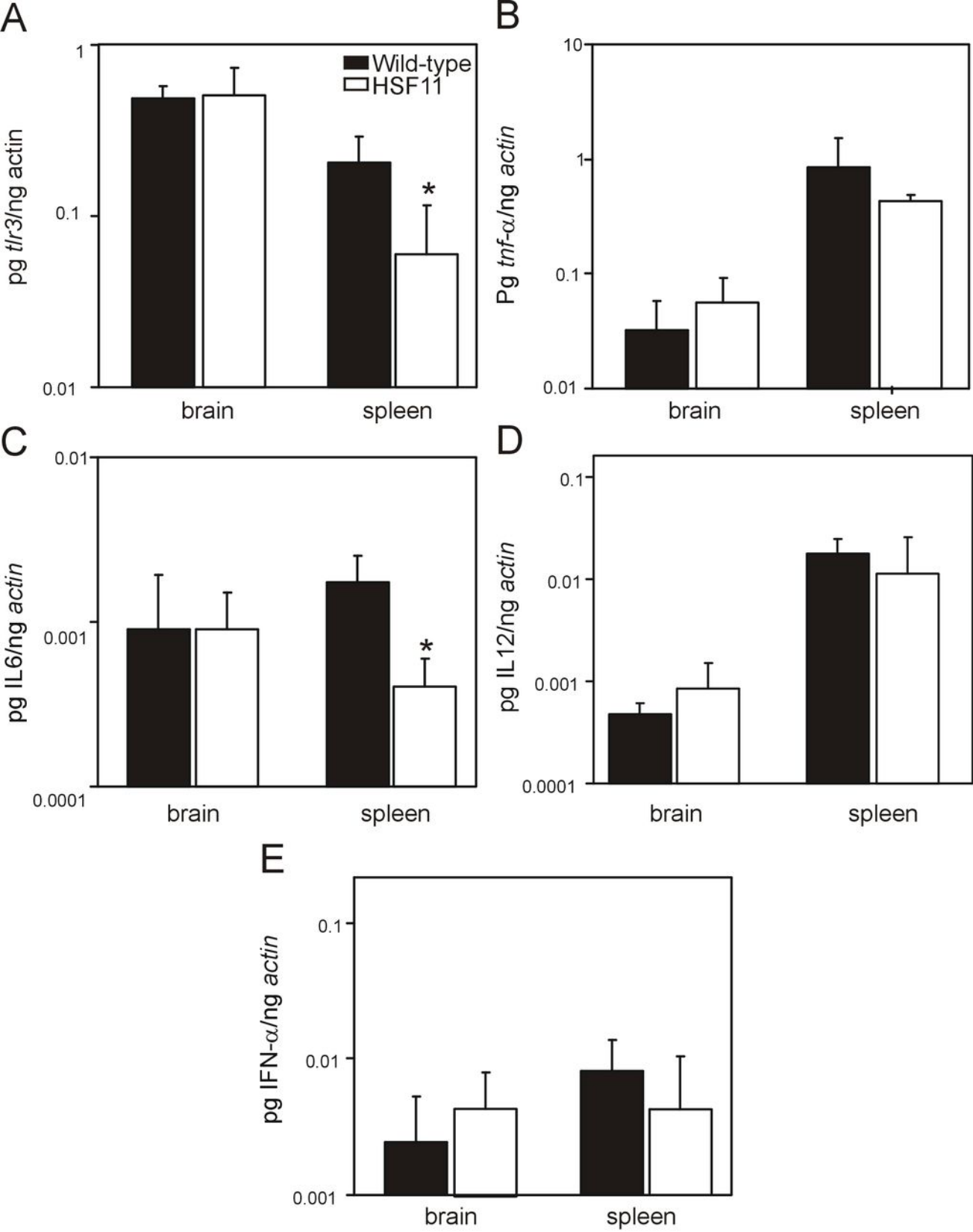
A
Wild-type
HSF11
pg tlr3/ng actin
1
0.1
0.01
*
brain
spleen
B
Pg tnf-α/ng actin
10
1
0.1
0.01
brain
spleen
C
pg IL6/ng actin
0.01
0.001
0.0001
*
brain
spleen
D
pg IL12/ng actin
0.1
0.01
0.001
0.0001
brain
spleen
E
pg IFN-α/ng actin
0.1
0.01
0.001
brain
spleen

Figure S3

Table S1: Oligonucleotides used in PCR and DNA sequencing

[a]: Oligonucleotide sequences are shown from 5' to 3' end. Oligonucleotides for sequencing of West Nile virus E-gene were designed based on the published sequences AF346315 and AF206518

[b]: relevant description and purpose of the primer usage is shown.

Sequence (5'-3')[a]	**Description[b]**
GGGGCAACGGCTGCGG	RT-PCR wild type
GGGGCAACGGCTGCGT	RT-PCR HSF11
TCAGCGATCTCTCCACCAAAG	E-gene, QRT-PCR
GGGTCAGCACGTTTGTCATTG	E-gene, QRT-PCR
AATATGCTGAAACGCGAGAGAAACCGCG	DENV2-Capsid gene, Q-RT-PCR
CTCTTCAGTATCCCTGCTGTTGG	DENV2-Capsid gene, Q-RT-PCR
CACTTAAAGAGTTCTCCCCGGG	TLR3, Q-RT-PCR
TTCAGTTGGGCGTTGTTCAA	TLR3, Q-RT-PCR
CTCCAGGCGGTGCCTATGT	TNF-α, Q-RT-PCR
GAAGAGCGTGGTGGCCC	TNF-α, Q-RT-PCR
CCAGAAACCGCTATGAAGTTCC	IL-6, Q-RT-PCR
TCACCAGCATCAGTCCCAAG	IL-6, Q-RT-PCR
CTCAGGATCGCTATTACAATTCCTC	IL-12, Q-RT-PCR
CCTAGGATCGGACCCTGCA	IL-12, Q-RT-PCR
CTTCCACAGGATCACTGTGTACCT	IFN-α, Q-RT-PCR
TTCTGCTCTGACCACCTCCC	IFN-α, Q-RT-PCR
CAGCCGTCATTGGTTGGAT	E-gene forward primer
ACGCAGCTGTCGCCTTCG	E-gene sequencing
AGAGGTCCGCAGTTATTGCT	E-gene sequencing
GTCAATGCTTCCTTTGCCA	E-gene sequencing
GAAGTGGCCATTTTTGTCCA	E-gene sequencing
TGTCAATCCCTGACCGTG	E-gene reverse primer
TCAACCTCCCTTGGAGCA	E-gene sequencing
AACTTGACAGTGTTGCTTGAAAA	E-gene sequencing
CTGTTCAAAGGCTTTCAAGTTTC	E-gene sequencing
CATTGAAACAAAAGGGTTGACA	E-gene sequencing
AGAGGAGAACAACAGATCAATCAC	E-gene sequencing
CTCCGAACACTTGATGGACA	E-gene sequencing
GGATGGGCATCAATGCTC	E-gene sequencing
TCCATCCAAGCCTCCACAT	E-gene sequencing

Table S2: mAb11 cross-reacts with other flaviviruses
(* Cross-reactivity: +++ excellent, ++ very good, + good, +/- poor, - negative); (IFA, Indirect immunofluorescence assay; WB, Western blotting; ELISA, Enzyme-Linked immunosorbent assay)

Viruses tested for mAb11 cross-reactivity	**Cross-reactivity assay**	**cross-reactivity***
West Nile virus	IFA, WB, ELISA	+++
Dengue virus serotype 1	IFA, WB, ELISA	+++
Dengue virus serotype 2	IFA, WB, ELISA	+++
Dengue virus serotype 3	IFA, WB, ELISA	+++
Dengue virus serotype 4	IFA, WB, ELISA	+++
Yellow fever virus	IFA	++
St. Louis encephalitis virus	IFA	++
Murray Valley encephalitis virus	IFA	++
Japanese encephalitis virus	IFA	+
Powassan virus	IFA	+/-
Tick borne encephalitis virus	WB	-
Venezuelan equine encephalitis virus	IFA	-
La Crosse virus	IFA	-
Western equine encephalitis	IFA	-
Vero cells	IFA (negative control)	-